Triplex Formation by Pyrene-Labelled Probes for Nucleic Acid Detection in Fluorescence Assays

Ineke Van Daele,[a] Niels Bomholt,[a] Vyacheslav V. Filichev,[a, b] Serge Van Calenbergh,[c] and Erik B. Pedersen*[a]

Triplex-forming homopyrimidine oligonucleotides containing insertions of a 2′–5′ uridine linkage featuring a pyrene moiety at the 3′-position exhibit strong fluorescence enhancement upon binding to double-stranded DNA through Hoogsteen base pairing. It is shown that perfect matching of the new modification to the base pair in the duplex is a prerequisite for strong fluorescence, thus offering the potential to detect single mutations in purine stretches of duplex DNA. The increase in the fluorescence signal was dependent on the thermal stability of the parallel triplex, so a reduction in the pH from 6.0 to 5.0 resulted in an increase in thermal stability from 25.0 to 55.0 °C and in an increase in the fluorescence quantum yield (Φ_F) from 0.061 to 0.179, while the probe alone was fluorescently silent ($\Phi_F = 0.001$–0.004). To achieve higher triplex stability, five nucleobases in a 14-mer sequence were substituted with α-L-LNA monomers, which provided a triplex with a T_m of 49.5 °C and a Φ_F of 0.158 at pH 6.0. Under similar conditions, a Watson–Crick-type duplex formed with the latter probe showed lower fluorescence intensity ($\Phi_F = 0.081$) than for the triplex.

Introduction

During the last decade, the sequencing of the human genome has led to a strong need in cytogenetic research and clinical diagnosis for the development of probes capable of detecting specific sequences of nucleic acids.[1,2] The demand for such assays stems from a need in clinics to reduce the time required in the detection of diseases. One way to solve this problem would be to develop assays capable of detecting nucleic acid sequences directly in the cell, without any amplification steps such as PCR. Triplex technology can be used in molecular and cellular biology to inhibit transcription initiation or elongation by competing with the binding of transcription factors or RNA polymerases to dsDNA (for reviews see refs. [3, 4]). Chemically modified triplex-forming oligonucleotides (TFOs) can induce genomic changes (either mutagenesis or recombination) in cell extracts and even in mice.[5,6] Formation of triplexes has been demonstrated within supercoiled dsDNA in living bacteria, and there are more potential triplex-forming sequences in genomes.[7] Analysis of human and mouse genomes has shown that homopurine sequences longer than 14 base pairs—suitable potential triplex-forming sequences—are nearly homogeneously distributed over the genome and represent about 2% of the entire genome.[8] By the use of such sequences, sequence-specific recognition of DNA on a chromosomal level without denaturation of dsDNA can be achieved.[9] Recently, it has been found that 97.8% of known human and 95.2% of known mouse genes have at least one potential site for triplex formation with a suitable 15-mer TFO in the promoter and/or transcribed gene regions.[10] A triplex is formed when a TFO binds to a homopurine/homopyrimidine DNA duplex in the major groove through the formation of Hoogsteen base pairs with the homopurine/homopyrimidine strand.[11] As this triplex formation is highly specific, it can be used for sequence-specific recognition of dsDNA, without its prior denaturation.[12]

In 2003, Hausmann et al.[13] introduced combinatorial oligonucleotide fluorescence in situ hybridisation (COMBO-FISH), which uses oligonucleotides (ONs) that form triple helices with intact duplexes to label chromosomes in a cell nucleus under nondenaturing conditions. However, one of the disadvantages is the use of nucleic acid probes possessing a fluorophore that is not sensitive enough to changes in the microenvironment, especially after hybridisation of the probe to the complement. This leads to a high background signal and the requirement to wash out excess fluorescent probes, which makes labelling very difficult. To overcome these problems, novel fluorescent modified nucleic acids are needed. Among the available fluorophores, pyrene and its derivatives are attractive fluorescent dyes, due to their inherent chemical and photochemical characteristics, rather long fluorescence lifetimes and sensitivity to the microenvironment.[14] Interesting properties have been re-

[a] Dr. I. Van Daele, N. Bomholt, Dr. V. V. Filichev, Prof. E. B. Pedersen
Nucleic Acid Center, Department of Physics and Chemistry
University of Southern Denmark
Campusvej 55, 5230 Odense M (Denmark)
Fax: (+45) 6615-8780
E-mail: ebp@ifk.sdu.dk

[b] Dr. V. V. Filichev
Institute of Fundamental Sciences, Massey University
Private Bag 11222, Palmerston North 5301 (New Zealand)

[c] Prof. S. Van Calenbergh
Laboratory for Medicinal Chemistry
Faculty of Pharmaceutical Sciences (FFW), Ghent University
Harelbekestraat 72, 9000 Ghent (Belgium)

Supporting information for this article is available on the WWW under http://www.chembiochem.org or from the author.

ported when pyrene units positioned to form clamps stack at the end of triple helices.[15,16] We are looking for an ON probe with the fluorophore incorporated in the middle of the sequence and displaying a very low fluorescence signal as a single-stranded ON. Upon hybridisation there should be a considerable increase in the fluorescence signal (positive signal) to indicate binding to the target.

Previous research in which a pyrene unit was attached to the 2′-position through different linkers studied the effects of binding to ssDNA or ssRNA. These modified oligomers showed increases in the fluorescence signals upon binding to ssRNA.[17–21] So far, no similar effects have been described for triplex formation.

Obika et al.[22] demonstrated that the presence of several 2′–5′-linkages in a 3′–5′ TFO strand led to stabilisation of triplexes. As this change in the phosphate backbone offers potential for the introduction of a pyrene unit at the 3′-position, we decided to synthesise a modified nucleoside with the fluorophore attached to the 3′-position through a short linker.

Here we present the synthesis of a novel pyrene-containing nucleoside monomer that exhibited a strong increase in fluorescence quantum yield (Φ_F) from 0.004 for a ssON to 0.061 for a corresponding triplex DNA after incorporation into the middle of 14-mer homopyrimidine ONs upon excitation at 350 nm and at pH 6.0. Under similar conditions, Φ_F for a fully matched antiparallel duplex was 0.036. Substitution of five native nucleobases with α-L-locked nucleic acid (α-L-LNA) monomers in a modified TFO led to further increases in fluorescence quantum yield, to 0.158 for a Hoogsteen-type triplex and to 0.081 for a Watson–Crick duplex. The fluorescent nucleoside for ON synthesis was prepared by click chemistry between 1-ethynylpyrene and 3′-azidomethyl-3′-deoxy-5-methyl-uridine and incorporated into several ONs. Thermal stabilities and fluorescence spectra of the different probes, also containing other nucleic acid analogues, such as twisted intercalating nucleic acids (TINAs) and α-L-LNAs and their corresponding duplexes and triplexes with complementary ssDNA/RNAs and dsDNAs, were examined (Scheme 2, below). Modelling was used as a tool to visualise the fluorescence properties observed.

Results and Discussion

The synthesis of phosphoramidite **4** (Scheme 1) started from compound **1**, which was obtained in 11 steps from 1,2-O-isopropylidine-α-D-xylofuranose in an overall yield of 17%.[23] The formation of the 1,4-triazole was performed in a microwave
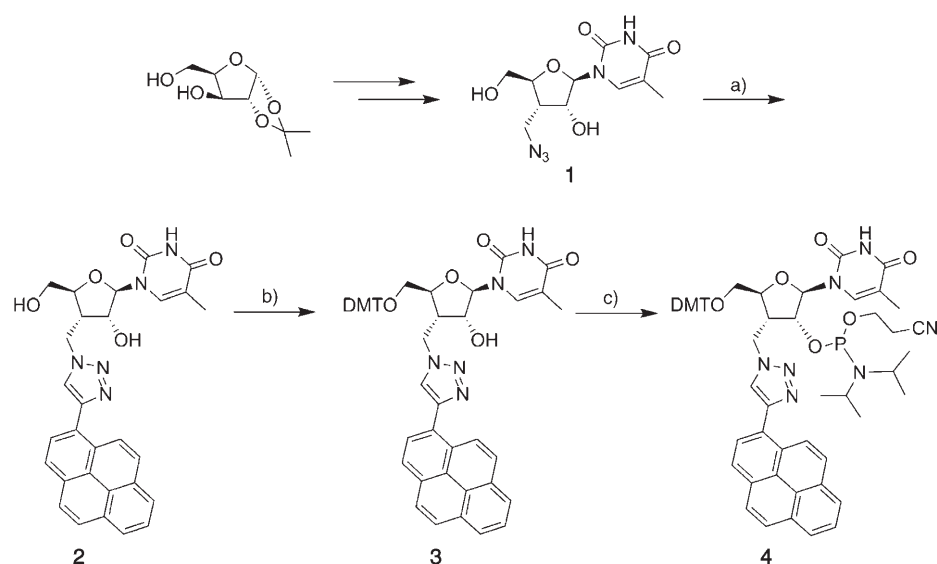
Scheme 1. Reagents and conditions: A) 1-ethynylpyrene, CuSO$_4$, ascorbic acid, DMF/H$_2$O 19:1, 15 min, 125 °C, microwave; B) DMT-Cl, pyridine, 16 h; C) NC(CH$_2$)$_2$OP(N^{i}Pr$_2$)$_2$, diisopropylammonium tetrazolide, CH$_2$Cl$_2$, 16 h.

cavity over 15 min at 125 °C in the presence of Cu^I as a catalyst in 79% yield. 5′-O-Dimethoxytrityl-protection followed by phosphitylation at the 2′-position were performed under standard conditions in 59% yield over two steps.

DNA synthesis of ONs with use of compound **4** was performed on a 0.2 μmol scale under standard conditions except for the use of an increased coupling time (10 min) and an extended deprotection step (100 s), with 4,5-dicyanoimidazole as an activator, which resulted in a coupling efficiency of 98%. The obtained ONs were purified by reversed-phase HPLC, their compositions were verified by MALDI-TOF (Table S1), and the purities were found to be over 82% by ion-exchange HPLC.

Hoogsteen base pairing

The thermal stabilities of triplexes and duplexes (DNA/DNA and DNA/RNA) formed with the synthesised oligonucleotides were determined by thermal denaturation studies. The melting temperatures (T_m, °C) determined as the first derivatives of the melting curves at 260 nm are listed in Table 1, and also in Tables 3 and 4, below.

For homopyrimidine sequences, pH-dependent Hoogsteen-type base pairing was studied, by determining the thermal stabilities of parallel triplexes toward duplex **D1** and of parallel duplexes toward **ON15** (Table 1). T_m values of Watson–Crick-type antiparallel duplexes formed by **ON1–10** and **ON16** are also shown. Since the latter type of duplexes can also be studied by mixed pyrimidine/purine sequences, mixed nonamer sequences were used for hybridisation with ssDNA and ssRNA (Table 4).

Obika et al.[22] described the stabilising effect of the discontinuous replacement of 3′,5′-phosphodiester linkages in TFOs by 2′,5′-linkages. As demonstrated by the T_m values for the **ON2/D1** and **ON5/D1** triplexes at pH 6.0, insertion of the fluorophore positioned at the 3′-carbon via a triazole linker tends

Table 1. T_m [°C] data for triplex and duplex melting of **ON1–10** with **D1**, **ON15** and **ON16**, Taken from UV melting curves ($\lambda = 260$ nm).

Sequence		Triplex[a] 3′-AAAAAAGAAAGGGGCAG 5′-TTTTTTCTTTCCCCGTC (**D1**)			Parallel duplex[b] 3′-AAAAAAGAAAGGGGCAG (**ON15**)			Antiparallel duplex[b] 5′-AAAAAAGAAAGGGG (**ON16**)		
		pH 5.0	pH 6.0	pH 7.2	pH 5.0	pH 6.0	pH 7.2	pH 5.0	pH 6.0	pH 7.2
ON1	3′-TTTTTTCTTTCCCC	55.0[d]	28.0	< 5.0	29.5	19.5	n.d.	47.5	48.5	47.0
ON2	3′-TTTTTTCT**X**TCCCC	55.0[c]	25.0	< 5.0	20.0	< 5.0	n.d.	45.0	47.5	45.5
ON3	3′-TTTTTTC**XX**TCCCC	33.0	19.5	n.d.[e]	32.0	21.5	n.d.	36.0	38.0	n.d.
ON4	3′-TTTTTTC**XXX**CCCC	32.0	< 5.0	n.d.	31.5	24.0	n.d.	36.5	38.5	n.d.
ON5	3′-TTTT**X**TCTTTCCCC	55.5[c]	16.0	n.d.	23.5	< 5.0	n.d.	39.5	43.0	n.d.
ON6	3′-TTTTTTC**X**TXCCCC	25.5	< 5.0	n.d.	21.5	< 5.0	n.d.	31.5	37.5	n.d.
ON7	3′-TTTT**X**TCTX**T**CCCC	27.0	< 5.0	n.d.	22.5	< 5.0	n.d.	34.5	39.5	n.d.
ON8	3′-TTTTTTCT**pX**TCCCC	54.0[c]	20.5	n.d.	27.5	16.5	n.d.	43.0	47.5	n.d.
ON9	3′-TTTTTTCT**Xp**TCCCC	53.0[c]	22.5	n.d.	29.0	20.0	n.d.	44.0	46.5	n.d.
ON10	3′-TT^{L}TTT^{L}TC^{L}TXTC^{L}CC^{L}C	65.5[d]	49.5[c]	35.5[c]	53.0	43.5	38.5	58.5	59.0	58.5

[a] p = TINA, T^L = thymin-1-yl α-L-LNA monomer, C^L = 5-methylcytosin-1-yl α-L-LNA monomer; Structure of monomer X is shown in Scheme 1 as the 5′-DMT-2′-phosphoramidite-derivative **4**, and structures of **p** and α-L-LNA are shown in Scheme 2; $C = 1.5$ μM of **ON1–10** and 1.0 μM of each strand of dsDNA (**D1**) in sodium cacodylate (20 mM), NaCl (100 mM), MgCl₂ (10 mM), pH 5.0, 6.0 and 7.2; duplex $T_m = 56.5$ °C (pH 5.0), 58.5 (pH 6.0) and 57.0 (pH 7.2). [b] $C = 1.0$ μM of each strand in sodium cacodylate (20 mM), NaCl (100 mM), MgCl₂ (10 mM), pH 5.0, 6.0 and 7.2. [c] Third strand and duplex melting overlaid; T_m was determined at 350 nm. [d] Third strand and duplex melting overlaid. [e] *n.d.* not determined.

to destabilise parallel triplexes. Introduction of a second 2′–5′-bonded 5-methyluridine with the pyrene residue led to further destabilisation of the parallel triplexes (**ON3**, **ON6**, **ON7** towards **D1**). Destabilisation was found to be higher for triplexes formed with **ON6** and **ON7**—with one or three nucleosides between two **X** units—than in the case for **ON3**, with two adjacent pyrene-containing uridines. Moreover, it is interesting to mention that at pH 5.0 the T_m value for the triplex with **ON4**, possessing three **X**s in a row, was higher than those for **ON6** and **ON7**, although all these values were lower than the T_m for the unmodified triplex. Such behaviour can be explained by the uninterrupted neighbouring 2′-5′-linkages in **ON4** in relation to the separate 2′-5′-linkages in **ON6** and **ON7**. This might also be a reason for the surprising stabilisation of parallel duplexes observed for **ON3** and **ON4** in comparison with the wild-type duplex **ON1/ON15** at pH 5.0 and 6.0 (Table 1). This is an interesting observation because both parallel triplexes and parallel duplexes are formed by Hoogsteen base pairing. However, a duplex, as a more flexible structure than a triplex, can more easily accommodate repetitive insertions of 2′–5′-bonded uridine linkages with pyrene in the middle of one of the strands. Unfortunately, this was not the case with Watson–Crick-type duplexes, with which drops in thermal stability were detected for **ON2**–**ON7** toward **ON16** in comparison with **ON1/ON16** at pH 5.0 and 6.0.

The presence of the pyrene residues in the ONs resulted in each case in the formation of an additional band, with a maximum at 350 nm, in their UV spectra. The single-stranded probes containing a single incorporation of the monomer **X** exhibited fluorescence with $\lambda_{max} \approx 386$ (band I) and 402 nm (band III) upon excitation at 350 nm. This emission appears at a higher wavelength than the typical pyrene monomer emission with $\lambda_{max} \approx 378$ (band I) and 391 nm (band III), which can be explained by the presence of the conjugated triazole ring in the monomer **X**. To our surprise, very low fluorescence intensities were observed for single-stranded ONs. Strikingly, the

formation of parallel triplexes caused huge increases in intensity (Figure 1 A and B). To study the fluorescence properties in greater detail we decided to determine fluorescence quantum yields (Φ_F) for ssONs and the corresponding complexes with complementary strands. Φ_F is defined as the ratio of the number of photons emitted by fluorescence at a certain wave-
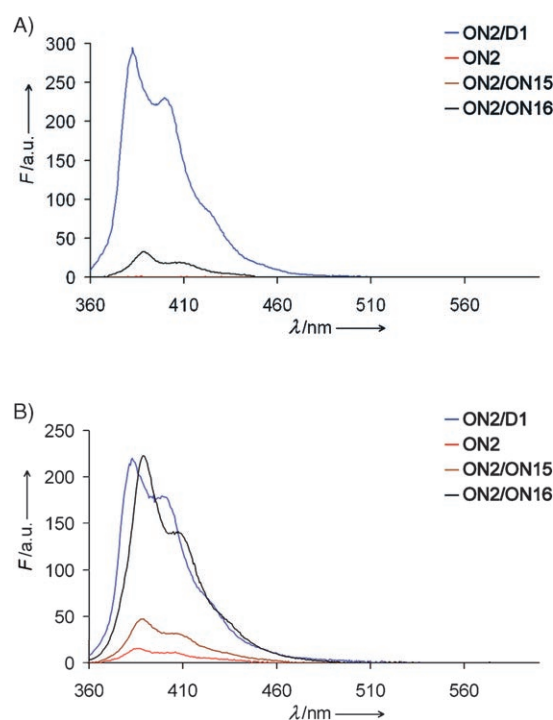

Figure 1. Steady-state fluorescence emission spectra of **ON2** and its corresponding complexes with **D1**, **ON15** and **ON16** upon excitation at 350 nm. Spectra of 1.0 μM solutions were recorded in thermal denaturation buffer at 10 °C at pH 5.0, emission slit 0.0 nm (Figure 1 A) and 10 °C at pH 6.0, emission slit 2.5 nm (Figure 1 B). In Figure 1 A, the curve of **ON2** overlaps that of **ON2/ON15** at the abscissa.

Table 2. Quantum yields at $\lambda = 350$ nm for single-stranded probes **ON2**, **ON5**–**ON7** and **ON10**, and the corresponding parallel triplexes and parallel and antiparallel duplexes in aerated thermal denaturation buffer at 10 °C.

Sequence		SS strand			Triplex[a] 3′-AAAAAAGAAAGGGGCAG 5′-TTTTTTCTTTCCCCGTC (D1)			Parallel duplex[a] 3′-AAAAAAGAAAGGGGCAG (ON15)			Antiparallel duplex[a] 5′-AAAAAAGAAAGGGG (ON16)		
		pH 5.0	pH 6.0	pH 7.2	pH 5.0	pH 6.0	pH 7.2	pH 5.0	pH 6.0	pH 7.2	pH 5.0	pH 6.0	pH 7.2
ON2	3′-TTTTTTCT**X**TCCCC	0.001	0.004	*n.d.*[b]	0.179	0.061	*n.d.*	0.001	*n.d.*	*n.d.*	0.032	0.036	*n.d.*
ON5	3′-TTTT**X**TCTTTCCCC	0.001	0.003	*n.d.*	0.138	0.023	*n.d.*	0.005	*n.d.*	*n.d.*	0.035	0.039	*n.d.*
ON6	3′-TTTTTTC**X**T**X**CCCC	0.001	0.003	*n.d.*	0.036	*n.d.*	*n.d.*	0.009	*n.d.*	*n.d.*	0.005	0.008	*n.d.*
ON7	3′-TTTT**X**TCT**X**TCCCC	0.002	0.003	*n.d.*	0.037	*n.d.*	*n.d.*	0.009	*n.d.*	*n.d.*	0.037	0.028	*n.d.*
ON10	3′-TT$^\text{L}$TTT$^\text{L}$TC$^\text{L}$T**X**TC$^\text{L}$CC$^\text{L}$C	0.001	0.003	0.05	0.179	0.158	0.073[c]	0.008	0.032	0.081[c]	0.046	0.081	0.038[c]

[a] T$^\text{L}$ = thymin-1-yl α-L-LNA monomer, C$^\text{L}$ = 5-methylcytosin-1-yl α-L-LNA monomer; C = 1.0 μM of each strand in sodium cacodylate (20 mM), NaCl (100 mM), MgCl$_2$ (10 mM), pH 5.0, 6.0 and 7.2. [b] *n.d.* not determined because of low thermal stabilities of triplexes. [c] Exciplex band at 460 nm was observed.

length to the number of photons absorbed at this wavelength. In our study, Φ_F was determined in the thermal denaturation buffer at 10 °C with use of equimolar quantities of each strand (1.0 μM) and excitation at 350 nm relative to anthracene ($\Phi_\text{F} = 0.36$) and 9,10-diphenylanthracene ($\Phi_\text{F} = 0.95$) in cyclohexane[24] by standard procedures (Table 2).[25, 26]

The fluorescence emitted by single-stranded **ON2** and **ON5**–**ON7** was strongly quenched, with Φ_F in a range from 0.001 to 0.004, which was most probably a result of communication with neighbouring bases including electron transfer.[27] Upon binding of these TFOs to the dsDNA (**D1**), increases in fluorescence intensity were detected at pH 5.0. As parallel triplexes are pH-sensitive and as more thermally stable complexes are formed under acidic conditions, due to required protonation of cytosine, fluorescence quantum yields were higher at pH 5.0 than at pH 6.0. For example, Φ_F for **ON2/D1** was almost three times higher in more acidic buffer (0.179 and 0.061 at pH 5.0 and 6.0, respectively). A correlation between the thermal stabilities of parallel triplexes and fluorescence quantum yields can also be illustrated by comparison of **ON2** and **ON5**. Thus, the T_m for **ON5/D1** at pH 6.0 was 9.0 °C lower than the T_m for **ON2/D1**, which resulted in a lower observed Φ_F value: 0.023 versus 0.061. Surprisingly large differences in fluorescence quantum yields between parallel triplexes and parallel or antiparallel duplexes formed by the same ON were observed. Almost complete quenching of fluorescence was detected for all parallel duplexes, even at pH 5.0, at which the complexes were most stable. Despite higher thermal stability, a lower Φ_F value for the antiparallel duplex **ON2/ON16** was observed than for the triplex **ON2/D1** at pH 6.0. The opposite situation was observed for another TFO with a single insertion of **X** (**ON5**) at the same pH: that is, $\Phi_\text{F(ON5/ON16)} > \Phi_\text{F(ON5/D1)}$, which was an outcome of low triplex thermal stability ($T_\text{m(ON5/D1)} = 16.0$ °C). With a reduction in the pH to 5.0, the fluorescence intensities of triplexes were much higher than those for antiparallel duplexes (see **ON2**, **ON5** and **ON6** toward **D1**; Table 2). All measurements of Φ_F were performed at 10 °C. Because of partial melting of parallel triplexes, lower Φ_F values were detected at 20 °C (results are not shown). To ensure that these effects were not a consequence of interactions of the pyrene residue in the structure

X with metal ions present in cacodylate buffer solution we performed measurements in medium-salt sodium phosphate buffer at pH 5.0 and observed the same tendency in the fluorescence spectra as described above upon binding of **ON2** to **D1**, **ON15** and **ON16** (results are not shown). Excimer bands were observed at 480 nm in the fluorescence spectra for triplexes formed by **ON3** and **ON4**, as a result of the placing of two and three adjacent pyrene uridines **X**, respectively, in the sequence. Because of this we did not consider these probes in the determination of fluorescent quantum yields for single-stranded probes and corresponding triplexes.

Discrimination in fluorescence properties upon binding of ONs possessing pyrene residues to dsDNA and to ssDNAs has never previously been reported. The strong increase in fluorescence intensity upon binding to dsDNA is a very important feature and an advantage of the described probe, as it offers novel potential for the detection of nucleic acids through triplex formation. Previously described attempts were devoted to the development of probes based on the principle of molecular beacons: that is, a fluorophore and a quencher were placed separately at the 3′- and 5′-ends of the TFO, which was extended with a number of complementary bases in order to make a hairpin and thus to position a fluorophore and a quencher in close proximity.[28] No signal was observed for the probe alone, but the presence of dsDNA resulted in hybridisation of the probe followed by increase in fluorescence intensity. However, it is known that molecular beacons can sometimes open up in the absence of complementary targets in cell media after entering the cell, bringing false positives in the detection assays.[29] Existing nucleic acid staining dyes, based on small molecules such as TOTO and others,[30] and which are used nowadays for labelling of dsDNA, have two main disadvantages. Firstly, such staining dyes bind to dsDNA unspecifically or have preferences only towards certain regions, which are usually repetitive in the genome.[31] Secondly, these dyes have very low affinities towards triplexes as a consequence of poorly fitting shapes of molecules to the base triplet and due to electrostatic repulsion between C$^+$-G-C triads and the positively charged structures of the dyes.[32] For that reason, a combination of a TFO and a free staining dye cannot be used for

sequence-selective labelling of dsDNA. Therefore, nucleic acid probes incorporating one or several modified nucleotide(s) containing a fluorophore that will give positive signals upon binding to complementary strands are of great importance for any detection technique. The main drawback of the monomer **X** is its destabilizing effect upon triplex formation. That is why attempts were made to develop a TFO capable of forming stable triplexes at the realistic cell pH values of 6.0 and 7.2 and at the same time showing the same favourable fluorescence intensity increases as observed for the ONs described above.

In **ON8** and **ON9**, we used bulged insertions of TINA monomer (Scheme 2), known to stabilise parallel triplexes with ΔT_m
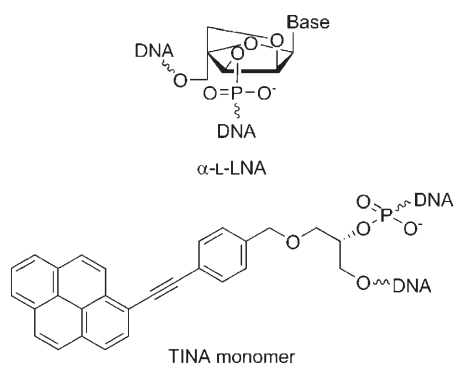
Scheme 2. Structures of the incorporated triplex stabilisers.

values of up to 19.0 °C for a single insertion of **p**.[33] A disadvantage of the TINA monomer in this particular case is that the excitation wavelengths for **X** and **p** are very close to each other—350 and 373 nm, respectively—meaning that irradiation of only one of these monomers is hardly achievable. We assumed that by placing **p** as a left or right bulged neighbour to the modification **X** in **ON2**, strong monomer fluorescence coming from TINA in a single-stranded state could be transferred to an excimer band appearing at longer wavelengths through the interaction of two pyrenes. In contrast with these expectations, further destabilisation of parallel triplexes was observed (Table 1; **ON8** and **ON9** towards **D1** in comparison with **ON2/D1** at pH 6.0). Moreover, high monomer fluorescence was detected for ss**ON8** and ss**ON9** with only very small excimer band at 480 nm upon excitation at 350 nm; this hampered the detection of binding these probes to dsDNA by fluorescence. However, these results do not exclude the use of TINA monomers in a combination with the monomer **X** in the future. For this purpose, fluorescently orthogonal intercalators to pyrene **X**, such as naphthalene derivatives,[33] should be used in the TINA structure and could be placed three or four bases away from **X** inserted in the TFO.

An alternative to intercalating nucleic acids is sugar-modified nucleotides, which are fluorescently silent and give thermal stabilisation upon insertion into TFOs. We decided to use α-L-LNA (Scheme 2), which stabilises triplexes up to 5 °C per modification. As a general rule, every third or fourth nucleotide in the TFO should be substituted by α-L-LNA monomer in order to achieve high T_m values at neutral pH.[34] Use of a 5-methylcy-

tosine derivative of α-L-LNA is also an advantage for parallel triplex formation, because 5-methylcytosine is more easily protonated than cytosine.[35] In the sequence **ON10**, five α-L-LNA nucleotides were incorporated, leading to increased thermal stability in all cases (Table 1). Thus, at pH 6.0 a triplex stabilisation of 5 °C per insertion of α-L-LNA was observed and at pH 7.2 the triplex **ON10/D1** melted at 35.5 °C. Parallel and antiparallel duplexes formed by **ON10** with **ON15** and **ON16**, respectively, were more thermally stable than the wild-type duplexes of **ON1**. Indeed, at pH 7.2 the parallel duplex **ON10/ON15** showed a higher T_m than the corresponding triplex **ON10/D1** with a ΔT_m value of $+3.0$ °C, which puts the formation of the triplex in question. In order to confirm the triplex formation of **ON10** with duplex **D1** we recorded CD spectra at different pH values (Figure 2). The negative band at ~212 nm
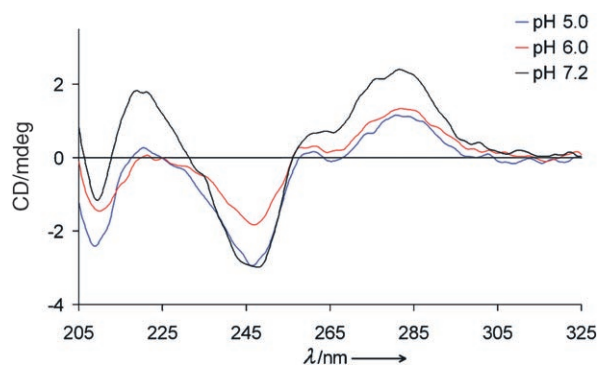

Figure 2. CD spectra of solutions of **ON10/D1** (1.0 μM) in thermal denaturation buffer at 10 °C at pH 5.0, 6.0 and 7.2.

is considered to be a sign of a parallel homopyrimidine DNA triplex[36] and it has also been observed for triplexes formed by α-L-LNA-modified TFOs.[34] As can be seen from Figure 2, a negative band at ~212 nm was present in the CD spectra at pH 5.0, 6.0 and 7.2, thereby confirming the formation of a triple helix for **ON10**. To ensure that the observed negative band at ~212 nm was exclusively representative of triplex formation we recorded CD spectra of the parallel duplex **ON10/ON15** and the target duplex **D1** at the same pH (Figure S5 and S6, respectively). No negative peak at ~212 nm was observed for the parallel duplex **ON10/ON15**, while higher intensity bands at ~220, ~245 and ~280 nm relative to the CD spectrum of **ON10/D1** were detected, thus confirming the formation of the triplex in this case. CD spectra of **D1** alone also showed a negative band at ~212 nm, but with a lower intensity than that seen with **ON10/D1**. On comparison of the CD spectra profiles of **ON10/D1** with increasing pH values, the CD spectrum of the triplex becomes similar to the CD spectrum of the corresponding duplex. Melting of the triplexes at pH 7.2 and 6.0 was therefore clearly seen in the CD spectra recorded at 40 °C and 55 °C, respectively (see Figure S3 in the Supporting Information).

With regard to the fluorescence properties of **ON10**, a similar increase in fluorescence intensity was observed upon triplex formation at pH 5.0 and 6.0 caused by monomer **X** (Figure 3).
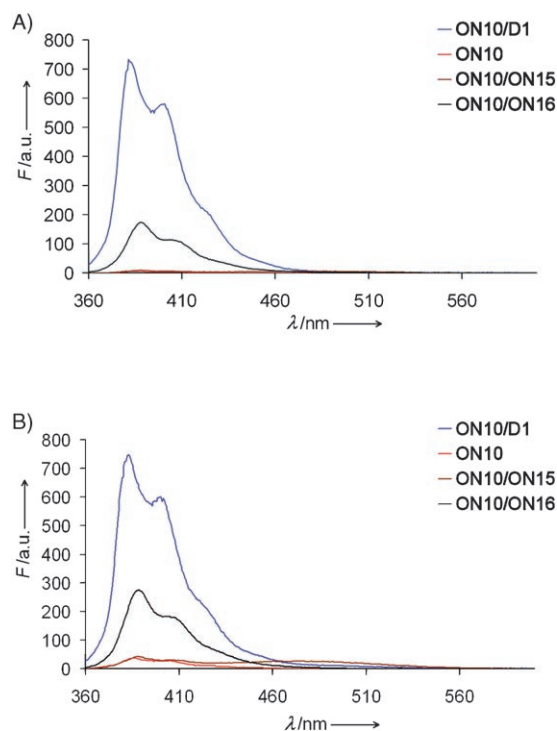
Figure 4. Steady-state fluorescence of ss**ON10** and its corresponding triplex with **D1**, and parallel and antiparallel duplexes with **ON15** and **ON16**, respectively. Spectra were recorded in thermal denaturation buffer at pH 7.2 at 10 °C, using an excitation wavelength of 350 nm.

Figure 3. Steady-state fluorescence of **ON10** and the corresponding complexes with **D1**, **ON15** and **ON16** upon excitation at 350 nm. Spectra of **ON** solutions (1.0 μM) were recorded in thermal denaturation buffer at 10 °C at pH 5.0 and 6.0, emission slit 2.5 nm (Figure 3 A and 3 B, respectively). In Figure 3 A, the curve of ss**ON10** overlaps the one of **ON10**/**ON15** at the abscissa.

Interestingly to note, there was the same value of fluorescence quantum yield (0.179) for triplexes formed by either **ON2** or **ON10** at pH 5.0 (Table 2). A considerably lower decrease in Φ_F was detected for **ON10**/**D1** than for **ON2**/**D1** upon changing the pH from 5.0 to 6.0, which is clearly a consequence of higher triplex thermal stability for **ON10**. Importantly, the fluorescence intensity for the antiparallel duplex **ON10**/**ON16** was lower than that for the corresponding triplex at pH 5.0 and 6.0, meaning that fluorescent discrimination between triplex and antiparallel duplex caused by **X** in **ON2** remained after substitutions of some natural bases in TFO by α-L-LNA.

At pH 7.2, the parallel duplex and triplex with **ON10** were less stable, due to the deprotonation of cytosine (Table 1). Moreover, the fluorescence intensity of the probe alone increased slightly upon changing of the pH from 5.0 to 6.0 and then to 7.2 (ss**ON10**; Figure 3 and 4). It is known that the band III/I ratio is affected by local environmental polarity,[37] and the observed changes in fluorescence were associated with changing of pH and deprotonation of cytosine. Upon binding of **ON10** to complementary dsDNA and ssDNAs a new broad emission appeared at longer wavelength (460 nm; Figure 4). However, it differed from an excimer emission band (480–500 nm), which is usually caused by interactions of at least two pyrene units positioned in closed proximity. Similar results have been observed by Yamana et al.[38] upon duplex formation of pyrene-labelled oligonucleotides. The increased band
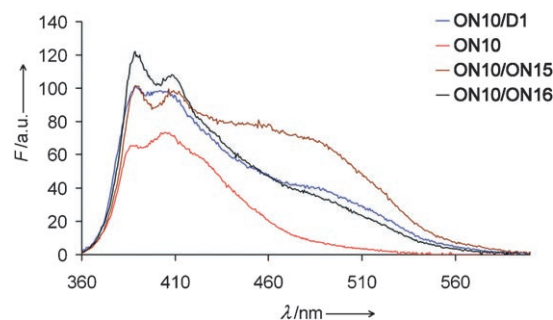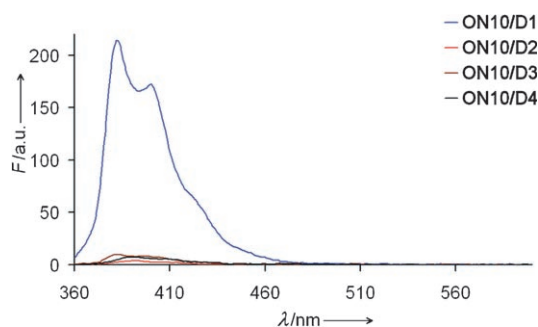
III/I intensity ratio was associated with a decrease in local environmental polarity. In our case the pyrene residue was most probably transferred into the more hydrophobic base-pair pocket, which led to a new broad emission band around 460 nm. This emission can be ascribed to the exciplex of the pyrene and an adjacent base. This effect was observed upon triplex formation, but was even more obvious in the fluorescence spectrum for the parallel duplex at pH 7.2 (Figure 4). The latter, as we have already mentioned above, is a less rigid structure than the triplex, thus providing extra room for interaction of pyrene with neighbouring bases.

In order to determine the effect when the duplex base pair does not match the modification in the TFO, the melting temperatures of triplexes formed by **ON2** and **ON10** with duplexes **D2**–**D4** were determined at pH 5.0 and 6.0 as shown in Table 3. As might be expected, the mismatched triplexes formed with **ON2** showed much lower thermal stabilities than the matched triplex **ON2**/**D1** ($\Delta T_m > -25.0$ °C), and no changes in the fluorescent spectra of ss**ON2** were observed upon its hybridisation to mismatched dsDNAs. The presence of the α-L-LNA in **ON10** resulted in the formation of considerably more stable mismatched triplexes than were obtained with **ON2**. Thus, at pH 5.0 the differences in T_m values for matched (**ON10**/**D1**) and mismatched (**ON10**/**D2**–**D4**) triplexes did not exceed 7.0 °C, showing the highest drop in T_m with duplex **D3**. Nevertheless, the formation of mismatched triplexes with **ON10** was confirmed by the presence of a negative band at ~212 nm in each of their CD spectra at 10 °C. T_m values obtained by UV were verified by monitoring changes in mdeg at 210 nm in CD against increased temperature, with the exception of **ON10**/**D4** at pH 6.0, where triplex formation could not be confirmed (Table 3 and Figure S7 B). Interestingly, at pH 5.0, despite the high thermal stabilities of triplexes **ON10**/**D2**–**D4**, where uridine **X** did not match with the duplex bases, we observed ~20-fold decreases in fluorescence intensity for all three mismatched triplexes relative to the perfectly matched **ON10**/**D1** (Figure 5; see Figure S2 for pH 6.0). High levels of fluorescence quenching and high thermal stabilities of mismatched triplexes with **ON10** might be a result of interaction of the pyrene moiety with adjacent nucleobases, which might occur if

Table 3. T_m [°C] data for mismatched parallel triplex of **ON2** and **ON10**, determined from UV melting curves ($\lambda = 260$ nm) and fluorescence quantum yields at 350 nm (in brackets).

	Sequence	3'-TTTTTTCTXTCCCC[a] (**ON2**)		3'-TT^{L}TTT^{L}TC^{L}TXTC^{L}CC^{L}C[a] (**ON10**)	
		pH 5.0	pH 6.0	pH 5.0	pH 6.0
D1	3'-AAAAAAGAAAGGGGCAG 5'-TTTTTTCTTTCCCCGTC	55.0[b]	25.0	65.5[c,d]	49.5[b,c]
D2	3'-AAAAAAGA**C**AGGGGCAG 5'-TTTTTTCT**G**TCCCCGTC	28.0 (0.001)	< 5.0	62.0[b,c]	41.5[b,c]
D3	3'-AAAAAAGA**G**AGGGGCAG 5'-TTTTTTCT**C**TCCCCGTC	21.0 (0.001)	< 5.0	58.5[b,c]	34.5[b,c]
D4	3'-AAAAAAGA**T**AGGGGCAG 5'-TTTTTTCT**A**TCCCCGTC	29.5 (0.001)	< 5.0	61.0[b,c]	40.5[b]

[a] T^L = thymin-1-yl α-L-LNA monomer, C^L = 5-methylcytosin-1-yl α-L-LNA monomer; for T_m measurement: $C = 1.5$ μM of **ON2** or **ON10** and 1.0 μM of each strand of matched and mismatched dsDNA in sodium cacodylate (20 mM), NaCl (100 mM), MgCl$_2$ (10 mM), pH 5.0 and 6.0; for quantum yield measurement: $C = 1.0$ μM of each strand in the same buffer at pH 5.0. [b] Third strand and duplex melting overlaid—T_m was determined at 350 nm. [c] T_m values obtained by UV were verified by monitoring changes in mdeg at 210 nm in CD against increased temperature. However, these melting temperatures are less well defined due to low concentrations (Figures S4 and S8). [d] Third strand and duplex melting overlaid.

which can be down to 6.4 for human cancers, and down to 6.12 for mouse cancers, depending on the tumour type.[39] Therefore, the described probe should be an appropriate platform for the development of sequence-specific detectors for tumour cells. Moreover, as COMBO-FISH experiments are currently performed under conditions with pH values of around 6.0,[13] probes based on the design of **ON10** are suitable for such experiments.

Watson–Crick base pairing

To study the influence of the monomer **X** on Watson–Crick base pairing, a mixed sequence with one, two or three incorporated neighbouring modified nucleotides was synthesised. Table 4 shows the thermal stabilities of **ON11–14** upon hybridisation to ssDNA/ssRNA and the fluorescence quantum yields for **ON12** and its complexes determined at 350 nm.

Upon hybridisation of **ON12** with ssDNA, a twofold increase in fluorescence intensity was observed. Binding to complementary ssRNA resulted in an approxi-

Figure 5. Steady-state fluorescence of **ON10** and the corresponding complexes with **D1–D4** upon excitation at 350 nm. Spectra of 1.0 μM dsDNA with 1.5 μM of **ON10** were recorded in thermal denaturation buffer at 10 °C at pH 5.0, emission slit 0.0 nm.

Table 4. T_m [°C] data for duplex melting of **ON11–14** and DNA/RNA complements, taken from UV melting curves ($\lambda = 260$ nm) and fluorescence quantum yields determined for **ON12**.

	Sequence	5'-GTGAAATGC[a] DNA (**ON17**)	5'-GUGAAAUGC[a] RNA (**ON18**)
ON11	3'-CACTTTACG	36.0	34.0
ON12	3'-CACT**X**TACG (0.02)[b]	20.0 (0.04)	19.0 (0.07)
ON13	3'-CACT**XX**ACG	< 5.0	13.5
ON14	3'-CAC**XXX**ACG	< 5.0	< 5.0

[a] Thermal denaturation temperatures measured as the maximum of the first derivative of the melting curve (A_{260} vs temperature) recorded in high-salt buffer (1400 mM NaCl, 20 mM sodium phosphate, pH 7.0) with 1.0 μM concentrations of each complementary strand. [b] Fluorescence quantum yields were measured in the aerated thermal denaturation buffer at 10 °C, with 1.0 μM concentrations of each complementary strands at an excitation wavelength of 350 nm.

pyrene moved from outside the triplex into the triplex interior. This is possible because of imperfect triplex base pairing and consequent repulsion of thymine at mismatched positions, making room for pyrene intercalation. The excellent discrimination in fluorescence for **ON2** and **ON10** observed between matched and mismatched triplexes can be used for detection of dsDNA through formation of perfectly matched parallel triplexes.

Although the formation of the exciplex bands for complexes of **ON10** at pH 7.2 was unexpected, it offers new potential for the use of this probe for diagnostic purposes. Fluorescence intensity upon hybridisation to dsDNA at pH 7.2 was much lower (about 100 a.u.; Figure 4) than that at pH 6.0 (750 a.u.; Figure 3). Such pH-dependent fluorescence signals can be useful for dsDNA detection in cells with lower pH values. Tumour cells have a natural tendency to overproduce acids, resulting in more acidic pH values in tumour microenvironments,

mately 3.5-fold increase in fluorescence intensity (Figure 6). Similar results have previously been described for 2'-pyrene-modified oligoribonucleotides. The 2'-N-positions in 2'-amino-DNA[17,18] and 2'-amino-LNA[19] or the 2'-O-positions in RNA[20,21] have been substituted with pyrene through a short tether. In these cases the increase in fluorescence upon hybridisation to ssRNA was considerably stronger than in the case of binding to ssDNA.

This short study of the influence of **X** on Watson–Crick base pairing shows that a much larger decrease in stability is obtained, while a smaller increase in fluorescence signal upon binding can be observed. Duplexes with RNA show higher increases than duplexes with DNA, similarly to previous reported analogue studies.
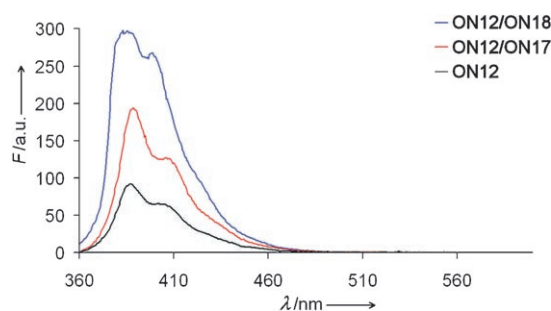
Figure 6. Steady-state fluorescence emission spectra of **ON12** and the corresponding duplexes with complementary ssDNA/RNA. Spectra were recorded in thermal denaturation buffer at 10 °C with use of an excitation wavelength of 350 nm and an excitation slit of 4.0 nm and emission slit of 2.5 nm.

Molecular modelling

Molecular modelling studies were performed on the complexation of a truncated dsDNA with **ON2** (3′-TTC T**X**T CCC-5′) in order to visualise different conformations of the pyrene-modified 2′-5′-bonded uridine (structure **X**). The parallel triplex was analysed with pyrene located either inside or outside of the triplex. As can be seen from comparing Figure 7 A and B, a larger distortion of the triplex structure was observed when the pyrene intercalated with the bases of the triplex. In agreement with our observation of very strong fluorescence signal for **ON2/D1**, Figure 7 B and C shows the projected conformation of the pyrene-modified 2′-5′ uridine. Despite distortion of the

triplex structure upon intercalation of pyrene, this was most probably the case for triplex **ON10/D1** at pH 7.2 when an exciplex band was observed in the fluorescence spectrum.

To explain the practically total quenching of fluorescence for ssONs possessing **X** we performed molecular modelling analysis of the truncated single-stranded **ON2** (3′-TTC T**X**T CCC-5′). Studies showed that on rotation of the modified nucleotide so that the pyrene moiety was situated between neighbouring nucleobases, the pyrene was able to stack with the nucleobases to give a fluorescently silent oligonucleotide (Figure 7 D). Upon hybridisation to complementary dsDNA, pyrene would be forced outside the triplex, thereby explaining the increase in the fluorescence signal observed for complexes of **ON2**, **ON5** and **ON10** with matched duplexes.

Modelling studies for the duplex formed between **ON12** and complementary ssDNA showed serious distortions of the phosphate backbone and Watson–Crick base pairs upon positioning of the pyrene moiety between bases of the dsDNA (Figure 7 E). The intercalation of pyrene led to a more stable duplex structure with an increase in stability of ∼1966 kJ mol^{-1} relative to the duplex with the pyrene moiety placed outside the duplex (Figure 7 F). However, the conformation with pyrene intercalated in the duplex can be rejected on the basis of our experimental results. The formation of a less stable duplex and an increase in the fluorescence signal upon hybridisation of **ON12** indicates, despite what the modelling studies might show, that the conformation of the duplex is the one in which the pyrene moiety is directed outside of the duplex.
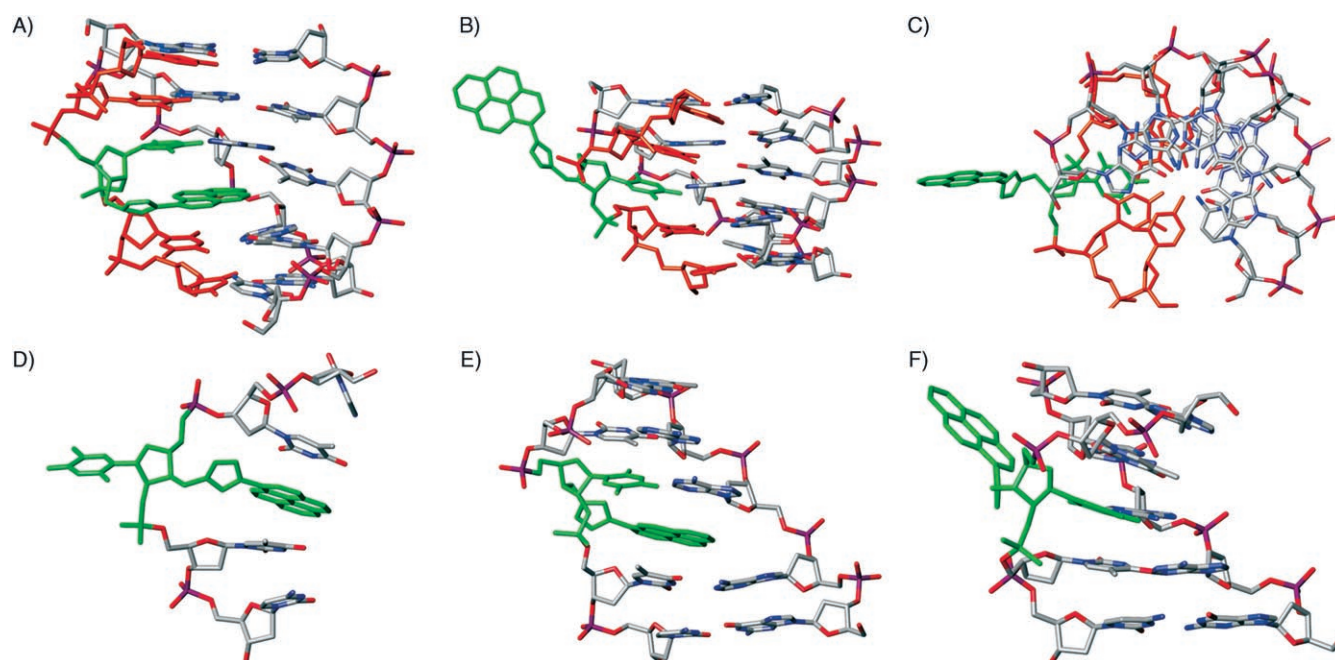

Figure 7. Representative truncated structures obtained by molecular modelling studies of the triplex, ssDNA and dsDNA. The modified nucleotide is shown in green and the TFO is shown in orange. A) Triplex formed by **ON2** with dsDNA with the pyrene moiety inside the triplex. B), C) The triplex formed by **ON2** with dsDNA with the pyrene moiety outside of the triplex (side view and top view, respectively). D) ssDNA, **ON2**, with the pyrene moiety placed between neighbouring nucleobases. E), F) The dsDNA formed by **ON12** with complementary DNA, with the pyrene moiety placed inside and outside the duplex, respectively.

Conclusions

In conclusion, we have synthesised a novel 3′- substituted *ribo*-uridine analogue possessing a pyrene moiety coupled to the sugar part through a triazolylmethyl linker, component **X**, which was incorporated as a 2′–5′-linker into different ONs. Thermal stability studies showed that single incorporation of **X** components in place of thymidine in the middles of ONs resulted in reductions of T_m values for either Watson–Crick- or Hoogsteen-type complexes. While the single-stranded homopyrimidine probes were fluorescently silent with quantum yields (Φ_Fs) of 0.001–0.004, formation of parallel triplexes with the complementary dsDNAs led to very strong increases in the fluorescence signals, with the values of Φ_F being in a range from 0.023 to 0.179 depending on the site of insertion and thermal stability. Lowering the pH resulted in higher thermal stabilities of Hoogsteen-type triplexes and higher fluorescence quantum yields. Antiparallel duplexes of the same probes had lower values of Φ_F than parallel triplexes under similar conditions. Molecular modelling of triplexes showed that the pyrene-containing residue at the 3′-position in the 2′–5′-bonded *ribo*-uridine can be positioned outside the triplex with minimal distortion of the complex.

To compensate for the low thermal stability induced by **X**, known triplex stabilisers were additionally incorporated into ONs. In a first attempt, phenylethynylpyrene glycerol (TINA) was incorporated as a neighbouring bulge to the modification **X**. However, neither stabilisation nor the previously detected fluorescence enhancement was observed in triplexes formed by these ONs. For this reason, α-L-LNA—a nonfluorescent nucleotide monomer—was used to stabilise triplexes. As a result of five substitutions of native nucleic bases with α-L-LNA in the homopyrimidine sequence possessing **X**, enhancements in thermal stability and fluorescent quantum yield were observed at pH 6.0 and 5.0 upon parallel triplex formation. This oligonucleotide had very weak fluorescence signal as a single-stranded probe, and marginal changes in fluorescence were observed upon formation of mismatched triplexes, in which uridine **X** did not match with the dsDNA bases. This means that fluorescence discrimination between homopurine dsDNA stretches and sequences with single base pair inversion is feasible. Upon binding to dsDNA at pH 6.0, a very specific 50-fold increase in the fluorescence signal was observed, being much stronger than that for the antiparallel duplex formed by the same probe. However, at pH 7.2 a lower increase in fluorescence in a combination with a shift to a longer wavelength, attributed to exiplex formation, was observed. This feature should allow this kind of probe to be used to detect species of dsDNA in tumour cell environments, as these are known to overproduce acids and to have lower pH values than normal cells.

For the first time, a pyrene-labelled oligonucleotide probe that explores the use of increases in fluorescence signals to discriminate between dsDNA and ssDNAs has been developed. This is a promising platform for further development of fluorescent probes capable of binding sequence-selectively to dsDNA without prior denaturation of the target and giving a positive signal upon hybridisation. Such probes have potential for use in fluorescence in vivo hybridisation under vital conditions and in living cells.

Experimental Section

General synthesis procedures: NMR spectra were recorded on a Varian Gemini 2000 spectrometer at 300 MHz for ^{1}H with TMS ($\delta = 0.00$ ppm) as an internal standard and at 75 MHz for ^{13}C with CDCl$_3$ ($\delta = 77.0$ ppm) or DMSO ($\delta = 39.44$ ppm) as internal standards. Accurate ion mass determinations of the synthesised compounds were performed with a 4.7 T Ultima Fourier transform (FT) mass spectrometer (Ion Spec, Irvine, CA). The $[M+Na]^+$ ions were peak-matched by use of ions derived from the 2,5-dihydroxybenzoic acid matrix. MALDI-TOF mass spectra of isolated oligodeoxynucleotides (ONs) were determined on a Voyager Elite biospectrometry research station (PerSeptive Biosystems). Thin-layer chromatography (TLC) analyses were carried out with use of TLC plates (60 F$_{254}$) purchased from Merck and were visualised under UV light (254 nm). The silica gel (0.040–0.063 mm) used for column chromatography was purchased from Merck. Solvents used for column chromatography were distilled prior to use, while reagents were used as purchased.

Melting temperature measurements: Melting profiles were measured on a Perkin–Elmer Lambda 35 UV/Vis spectrometer fitted with a PTP-6 temperature programmer. The triplexes were formed by first mixing the two strands of the Watson–Crick duplex, each at a concentration of 1.0 μM, followed by the addition of the TFO at a concentration of 1.5 μM in the corresponding buffer solution. The solution was heated to 80 °C for 5 min and afterwards cooled to 15 °C and kept at this temperature for 30 min. The duplexes were formed by mixing the two strands, each at a concentration of 1.0 mM in the corresponding buffer solution, followed by heating to 80 °C for 5 min, and cooling to room temperature. The absorbances of both triplexes and duplexes were measured at 260 nm from 5 to 70 °C with a heating rate of 1.0 °C min^{-1}. Use of a slower heating rate (0.5 °C min^{-1}) resulted in the same melting curves. Control experiments were also performed at 350 nm for **ON2**. The melting temperatures (T_ms, °C) were determined as the maxima of the first derivative plots of the melting curves. All melting temperatures are within ±0.5 °C uncertainty as determined by repetitive experiments.

Fluorescence measurements: Fluorescence measurements were performed on a Perkin–Elmer LS-55 luminescence spectrometer fitted with a Julabo F25 temperature controller and with use of quartz optical cells with a pathlength of 1.0 cm. The spectra were recorded at 10 °C in the same buffer as for T_m studies, with use of 1.0 μM concentrations of each ON, except for **ON10** mismatch studies, in which a 1.5 μM concentration of **ON10** was used. In all cases, the absorption of the solutions in the range from 360 to 600 nm did not exceed 0.10, in order to avoid inner-filter effects, and was never less than 0.01, to avoid uncertainties. Corrections were made for solvent background. Steady-state fluorescence emission spectra (360–600 nm) were obtained as averages of five scans with an excitation wavelength of 350 nm, excitation slit of 4.0 nm, emission slit of 2.5 nm or 0.0 nm (slit not completely closed) and scan speed of 120 nm min^{-1}. For quantum yield determination, see the Supporting Information.

CD measurements: CD measurements were performed on a Jasco J-815 CD spectrometer fitted with a Jasco CDF-426S/15 temperature controller in quartz optical cells with a pathlength of 0.5 cm. The spectra were recorded in the same buffer as used for

T_m studies for **ON10** towards **D1** and **ON15** with 1.0 μM concentrations of each ON. In studies of the mismatched triplexes we used a 1.0 μM concentration of the dsDNA and a 1.5 μM concentration of **ON10**. In all cases, CD spectra were obtained with 100 mdeg sensitivity in the range from 205 to 325 nm with a data pitch of 0.1 nm. The spectra were taken as averages of five scans, corrected for solvent background and smoothed with 25 point moving average. CD-T_m measurements were recorded with 100 mdeg sensitivity and a temperature slope of $1\,^\circ\text{C min}^{-1}$ from $10\,^\circ\text{C}$ to $70\,^\circ\text{C}$ and a data pitch of $0.1\,^\circ\text{C}$, at 210 nm. Spectra were smoothed with 99 point moving average.

Synthesis of 1-{3-[(4-(pyren-1-yl)-1H-1,2,3-triazol-1-yl)methyl]-3-deoxy-β-D-ribofuranosyl}thymine (2): Freshly prepared aq. CuSO$_4$ (1 M, 283 μM, 0.28 mmol) was added to a solution of compound **1** (420 mg, 1.41 mmol) in a DMF/H$_2$O mixture (19:1, 8 mL) in a microwave tube. The solution was bubbled with Ar for 1 min. Afterwards, a freshly prepared aqueous sodium ascorbate solution (424 μM, 0.42 mmol) and 1-ethynylpyrene (480 mg, 2.12 mmol, dissolved in DMF/H$_2$O (19:1, 8 mL) were added. The mixture was again bubbled with Ar for 3 min. The resulting mixture in a sealed microwave tube was placed in an Emrys Creator microwave synthesiser. The heating temperature was set to $125\,^\circ\text{C}$, with a 30 s premixing time. The reaction mixture was irradiated for 15 min followed by N$_2$ cooling to $40\,^\circ\text{C}$. Afterwards, water was added and the mixture was kept at $6\,^\circ\text{C}$ for 5 h for complete precipitation of the formed triazole and unreacted alkyne. The precipitate was filtered off and washed with water to remove all catalysts. After this, the solid on the filter was washed with methanol to dissolve the triazole. The collected methanol was evaporated to dryness, and the residue was purified by silica gel column chromatography (CH$_2$Cl$_2$/MeOH 95:5) to yield the pure triazole **2** (583 mg, 79%). ^{1}H NMR (300 MHz, DMSO): $\delta = 1.79$ (s, 3H; 5-CH$_3$), 2.96 (m, 1H; H-3'), 3.51 (d, $J = 12.3$ Hz, 1H; H-5$_a$'), 3.81 (d, $J = 12.6$ Hz, 1H; H-5$_b$'), 4.19 (m, 1H; H-4'), 4.32 (m, 1H; H-2'), 4.67 (dd, $J = 6.0$ and 14.1 Hz, 1H; 3'-CH$_a$), 4.81 (dd, $J = 7.5$ and 14.1 Hz, 1H; 3'-CH$_b$), 5.33 (br s, 1H; 5'-OH), 5.78 (br s, 1H; 2'-OH), 6.24 (d, $J = 5.1$ Hz, 1H; H-1'), 8.04–8.41 (m, 9H; pyrene-H and H-6), 8.77 (s, 1H; triazole-H), 8.91 (d, $J = 6.3$ Hz, 1H; pyrene-H), 11.31 ppm (br s, 1H; NH); ^{13}C NMR (75 MHz, CDCl$_3$): $\delta = 12.24$ (5-CH$_3$), 41.17 (C-3'), 46.10 (3'-CH$_2$), 60.12 (C-5'), 74.80 (C-2'), 82.77 (C-4'), 90.87 (C-1'), 108.30 (C-5), 123.86, 124.24, 124.89, 125.04, 125.10, 125.38, 125.46, 126.41, 127.01, 127.27, 127.43, 127.61, 127.92, 130.31, 130.49, 130.87 (pyrene and triazole C-5), 136.14 (C-6), 146.03 (triazole C-4), 150.39 (C-2), 163.80 ppm (C-4); HR-ESI-MS: m/z: calcd for C$_{29}$H$_{25}$N$_5$O$_5$Na [M+Na]$^+$: 546.1753; found: 546.1769.

Synthesis of 1-{3-deoxy-5-O-(4,4'-dimethoxytriphenylmethyl-3-[(4-(pyren-1-yl)-1H-1,2,3-triazol-1-yl)methyl]-β-D-ribofuranosyl}-thymine (3): Compound **2** (530 mg, 1.01 mmol) was coevaporated three times with pyridine and dissolved in anhydrous pyridine (4 mL). 4,4'-Dimethoxytrityl chloride (461 mg, 1.36 mmol) was added under N$_2$. After 16 h, MeOH (0.5 mL) and EtOAc (20 mL) were added and the mixture was extracted with NaHCO$_3$ (20 mL). The water layer was extracted twice with EtOAc (20 mL). The combined organic layers were dried over MgSO$_4$, the MgSO$_4$ was filtered off, and the filtrate was evaporated to dryness and purified by column chromatography (CH$_2$Cl$_2$/MeOH/pyridine 97:2.5:0.5). Compound **3** (760 mg, 91%) was obtained as a yellow foam. ^{1}H NMR (300 MHz, CDCl$_3$): $\delta = 1.42$ (s, 3H; 5-CH$_3$), 3.10 (m, 1H; H-3'), 3.29 (m, 2H; H-5$_a$' and H-5$_b$'), 3.67 (s, 6H; 2 × OCH$_3$), 4.39 (m, 3H; H-2', 3'-CH$_2$), 4.71 (m, 1H; H-4'), 5.71 (m, 2H; H-1' and 2'-OH), 6.79 (d, $J = 8.7$ Hz, 4H; DMT), 7.15–7.43 (m, 10H; DMT and H-6), 7.72 (s, 1H; triazole-H), 7.89–8.10 (m, 8H; pyrene-H), 8.61 (d, $J =$

9.3 Hz, 1H; pyrene-H), 10.91 ppm (br s, 1H; NH); ^{13}C NMR (75 MHz, CDCl$_3$): $\delta = 12.06$ (5-CH$_3$), 42.86 (C-3'), 49.69 (3'-CH$_2$), 55.11 (OCH$_3$), 72.57 (C-2'), 75.95 (C-5'), 82.01 (C-4'), 87.53 and 87.08 (C-1' and C-(Ar$_3$)), 110.64 (C-5), 113.35, 124.93–131.28, 135.40 (pyrene, DMT and triazole C-5), 136.11 (C-6), 144.18 (triazole C-4), 146.55 (DMT), 150.58 (C-2), 158.70 (DMT), 164.55 ppm (C-4); HR-ESI-MS: m/z: calcd for C$_{50}$H$_{43}$N$_5$O$_7$Na [M+Na]$^+$: 848.3060; found: 848.3084.

Synthesis of 1-{2-O-[2-cyanoethoxy(diisopropylamino)-phosphino]-3-deoxy-5-O-4,4'-dimethoxy-triphenylmethyl-3-[(4-(pyren-1-yl)-1H-1,2,3-triazol-1-yl)methyl]-β-D-ribofuranosyl}-thymine (4): Compound **3** (510 mg, 0.62 mmol) was dissolved under N$_2$ in anhydrous CH$_2$Cl$_2$ (10 mL). N,N-Diisopropylammonium tetrazolide (159 mg, 0.93 mmol) was added, followed by the dropwise addition of 2-cyanoethyl tetraisopropylphosphordiamidite (223 mg, 0.74 mmol) with external cooling with an ice/water bath. After 16 h, the reaction was quenched with H$_2$O (6 mL). The layers were separated and the organic phase was washed with H$_2$O (6 mL). The water layers were washed with CH$_2$Cl$_2$ and the resulting organic phases were combined, dried over MgSO$_4$ and filtered. The solvent was removed under reduced pressure, and the residue was purified by silica gel column chromatography (CHCl$_3$/MeOH/pyridine 99:0.5:0.5). The purified compound **4** (412 mg, 65%) was obtained as a foam that was used in DNA synthesis. ^{1}H NMR (300 MHz, CDCl$_3$): $\delta = 1.19$–1.29 [m, 12H; 2 × CH(CH$_3$)$_2$], 1.40, 1.44 (s, 3H; 5-CH$_3$), 2.45 (t, $J = 6.0$ Hz, 2H; CH$_2$CN), 2.71 [m, 2H; 2 × CH(CH$_3$)$_2$], 3.27 (m, 2H; H-5$_a$' and H-5$_b$'), 3.64, 3.67 (s, 6H; 2 × OCH$_3$), 3.70 (m, 1H; H-3'), 4.09 (m, 1H; H-2'), 4.39 (m, 2H; 3'-CH$_2$), 4.71 (m, 1H; H-4'), 6.09, 6.14 (d, $J = 0.9$ Hz, 1H; H-1'), 6.76 (m, 4H; DMT), 7.17–7.41 (m, 10H; DMT and H-6), 7.70 and 7.77 (s, 1H; triazole-H), 7.94–8.22 (m, 8H; pyrene-H), 8.67, 8.72 ppm (d, $J = 9.3$ Hz, 1H; pyrene-H); ^{31}P NMR (CDCl$_3$): $\delta = 148.40$, 150.34 ppm in a ratio of 2:3; HR-ESI-MS: m/z: calcd for C$_{59}$H$_{61}$N$_7$O$_8$P [M+Na]$^+$: 1026.4318; found: 1026.4338.

Synthesis and purification of modified oligonucleotides: DMT-on oligodeoxynucleotides were synthesised in a 0.2 μmol scale on CPG supports with the aid of an Expedite Nucleic Acid Synthesis System Model 8909 (Applied Biosystems). Standard procedures were used for phosphoramidite **4** with 4,5-dicyanoimidazole as an activator except for the use of an extended coupling time (10 min) and an increased deprotection time (100 s), resulting in stepwise coupling yields of 98% for monomer **4** and >99% for unmodified DNA phosphoramidites.

The obtained DMT-on oligonucleotides bound to CPG supports were treated with aqueous ammonia (32%, 1.3 mL) at room temperature for 2 h and then at $55\,^\circ\text{C}$ overnight. Purification of the 5'-O-DMT-on ONs was carried out by reversed-phase semipreparative HPLC on a Waters Xterra MS C$_{18}$ column. DMT groups were cleaved by treatment with aq. AcOH (80%, 100 μL) for 20 min, followed by addition of H$_2$O (100 μL) and aq NaOAc (3 M, 50 μL). The ONs were precipitated from EtOH (99%, 600 μL). The precipitate was washed with chilled aqueous ethanol (70%). The purities of the obtained ONs were checked by ion-exchange chromatography on a LaChrom system (Merck Hitachi) with a GenPak-Fax column (Waters) and were found to be 100% for all ONs, except for **ON14**, which was 82%.

Molecular modelling: Molecular modelling experiments were performed with MacroModel v9.1 from Schrödinger. All calculations were conducted with the AMBER* force field and the GB/SA water model. The dynamics simulations were performed with stochastic dynamics, a SHAKE algorithm to constrain bonds to hydrogen, time step 1.5 fs and simulation temperature of 300 K. Simulation

for 0.5 ns with an equilibration time of 150 ps generated 250 structures, which were all minimised by the PRCG method with a convergence threshold of 0.05 kJ mol^{-1}. The minimised structures were examined with Xcluster from Schrödinger, and representative low-energy structures were selected. The starting structures were generated with Insight II v97.2 from MSI, followed by incorporation of the modified nucleoside building block.

Acknowledgements

[1] L. E. Morrison, *J. Fluoresc.* **1999**, *9*, 187–196.

[2] L. J. Kricka, *Ann. Clin. Biochem.* **2002**, *39*, 114–129.

[3] M. Faria, C. Giovannangeli, *J. Gene Med.* **2001**, 3, 299–310.

[4] K. M. Vasquez, P. M. Glazer, *Q. Rev. Biophys.* **2002**, *35*, 89–107.

[5] M. M. Seidman, P. M. Glazer, *J. Clin. Invest.* **2003**, 112, 487–494.

[6] K. M. Vasquez, L. Narayanan, P. M. Glazer, *Science* **2000**, *290*, 530–533.

[7] R. Zain, J. S. Sun, *Cell. Mol. Life Sci.* **2003**, 60, 862–870.

[8] M. Hausmann, C. Cremer, G. Linares-Cruz, T. C. Nebe, K. Peters, A. Plesch, J. Tham, M. Vetter, M. Werner, *Cell. Oncol.* **2004**, 26, 119–124.

[9] J.-S. Sun, J.-C. François, T. Montenay-Garestier, T. Saison-Behmoaras, V. Roig, N. T. Thuong, C. Hélène, *Proc. Natl. Acad. Sci. USA* **1989**, *86*, 9198–9202.

[10] Q. Wu, S. S. Gaddis, M. C. MacLeod, E. F. Walborg, H. D. Thames, J. DiGiovanni, K. M. Vasquez, *Mol. Carcinog.* **2007**, 46, 15–23.

[11] G. Felsenfeld, D. R. Davies, A. Rich, *J. Am. Chem. Soc.* **1957**, *79*, 2023–2024.

[12] I. Radhakrishnan, D. J. Patel, *Biochemistry* **1994**, *33*, 11405–11416.

[13] M. Hausmann, R. Winkler, G. Hildenbrand, J. Finsterle, A. Weisel, A. Rapp, E. Schmitt, S. Janz, C. Cremer, *BioTechniques* **2003**, *35*, 564–577.

[14] J. B. Birks, *Photophysics of Aromatic Molecules*, Wiley, London, **1970**.

[15] I. Trkulja, R. Häner, *J. Am. Chem. Soc.* **2007**, *129*, 7982–7989.

[16] I. Trkulja, R. Häner, *Bioconjugate Chem.* **2007**, *18*, 289–292.

[17] N. Kalra, M. C. Parlato, V. S. Parmar, J. Wengel, *Bioorg. Med. Chem. Lett.* **2006**, *16*, 3166–3169.

[18] N. Kalra, B. R. Babu, V. S. Parmar, J. Wengel, *Org. Biomol. Chem.* **2004**, *2*, 2885–2887.

[19] P. J. Hrdlicka, B. R. Babu, M. D. Sørensen, N. Harrit, J. Wengel, *J. Am. Chem. Soc.* **2005**, *127*, 13293–13299.

[20] K. Yamana, H. Zako, K. Asazuma, R. Iwase, H. Nakano, A. Murakami, *Angew. Chem.* **2001**, *113*, 1138–1140; *Angew. Chem. Int. Ed.* **2001**, *40*, 1104–1106.

[21] V. A. Korshun, D. A. Stetsenko, M. J. Gait, *J. Chem. Soc. Perkin Trans. 1* **2002**, 1092–1104.

[22] S. Obika, A. Hiroto, O. Nakagawa, T. Imanishi, *Chem. Commun.* **2005**, 2793–2795.

[23] V. Vanheusden, H. Munier-Lehmann, M. Froeyen, L. Dugué, A. Heyerick, D. De Keukeleire, S. Pochet, R. Busson, P. Herdewijn, S. Van Calenbergh, *J. Med. Chem.* **2003**, *46*, 3811–3821.

[24] I. B. Berlman, *Handbook of Fluorescence Spectra of Aromatic Molecules*, Academic Press, New York, **1965**.

[25] J. V. Morris, M. A. Mahaney, J. R. Huber, *J. Phys. Chem.* **1976**, *80*, 969–974.

[26] H. Du, R. A. Fuh, J. Li, A. Corkan, J. S. Lindsey, *Photochem. Photobiol.* **1998**, *68*, 141–142.

[27] M. Manoharan, K. L. Tivel, M. Zhao, K. Nafisi, T. L. Netzel, *J. Phys. Chem.* **1995**, *99*, 17461–17472.

[28] T. Antony, T. Thomas, L. H. Sigal, A. Shirahata, T. J. Thomas, *Biochemistry* **2001**, *40*, 9387–9395.

[29] R. W. Dirks, C. Molenaar, H. J. Tanke, *Histochem. Cell Biol.* **2001**, *115*, 3–11.

[30] T. L. Netzel, K. Nafisi, M. Zhao, J. R. Lenhard, I. Johnson, *J. Phys. Chem.* **1995**, *99*, 17936–17947.

[31] J. P. Jacobsen, J. B. Pedersen, L. F. Hansen, D. E. Wemmer, *Nucleic Acids Res.* **1995**, *23*, 753–760.

[32] M. D. Keppler, P. L. James, S. Neidle, T. Brown, K. R. Fox, *Eur. J. Biochem.* **2003**, *270*, 4982–4992.

[33] V. V. Filichev, E. B. Pedersen, *J. Am. Chem. Soc.* **2005**, *127*, 14849–14858.

[34] N. Kumar, K. E. Nielsen, S. Maiti, M. Petersen, *J. Am. Chem. Soc.* **2006**, *128*, 14–15.

[35] L. E. Xodo, G. Manzini, F. Quadrifoglio, G. A. Vandermarel, J. H. van Boom, *Nucleic Acids Res.* **1991**, *19*, 5625–5631.

[36] G. Manzini, L. E. Xodo, D. Gasparotto, F. Quadrifoglio, G. A. van der Marel, J. H. van Boom, *J. Mol. Biol.* **1990**, *213*, 833–843.

[37] K. Kalyanasundaram, J. K. Thomas, *J. Am. Chem. Soc.* **1977**, *99*, 2039–2044.

[38] K. Yamana, R. Iwase, S. Furutani, H. Tsuchida, H. Zako, T. Yamaoka, A. Murakami, *Nucleic Acids Res.* **1999**, *27*, 2387–2392.

[39] R. J. Gillies, N. Raghunand, G. S. Karczmar, Z. M. Bhujwalla, *J. Magn. Reson. Imaging* **2002**, *16*, 430–450.